Complex free surface flows for mould filling using centrifugal casting

McBride, D.; Humphreys, N. J.; Croft, T. N.; Green, N. R.; Cross, M.

Title of Publication *Edited by*
TMS (The Minerals, Metals & Materials Society), Year

COMPLEX FREE SURFACE FLOWS FOR MOULD FILLING USING CENTRIFUGAL CASTING

D. McBride[1], N. J. Humphreys[2], T. N. Croft[1], N. R. Green[2] and M. Cross[1]

[1]School of Engineering, Swansea University, Singleton Park, Swansea, Wales, UK
[2]School of Metallurgy and Materials, University of Birmingham, Edgbaston, Birmingham, UK

Keywords: Centrifugal Casting, Computational Modelling, Free Surface Simulation, Water Experiments

Abstract

A challenging application in the computational modelling of free-surface flows and interacting physical phenomena is in the context of centrifugal casting. The combination of complex rotating geometries, significant centrifugal forces and high velocity transient free surface flows, coupled with heat transfer and solidification yields a comprehensive problem. Obviously the objective in centrifugal casting is to capitalise on the resulting centrifugal forces to control the flow dynamics and reduce component defects.

This contribution will describe the enhancements required to enable conventional free surface algorithms to capture the details of the flow during the filling stage of centrifugal casting in what are inevitably complex three dimensional geometries. The work described in this paper concentrates on resolving the fluid film formation at the early filling stages and the subsequent vortex formation.

Validation of the above phenomena is a key issue; a series of water model experiments has been performed and recorded using high-speed video image capture. The objective was to validate and refine the computational model predictions using repeatable high quality experimental data, before application of the model in analysing full-scale centrifugal casting process. A number of key observations arise from this work that are not trivial to capture within the computational modelling tools; however, for the models to be useful in the analysing the full scale casting process, such physics must be reflected within their predictive capability.

Introduction

The combination of free surface flows in complex geometries coupled with centrifugal forces, heat transfer and solidification makes this a significant computational modelling challenge. There is now a suite of shape casting processes that involve rotating moulds to utilise the resulting centrifugal forces to control the flow dynamics and reduce the defects. The defects arise as a consequence of :- air remaining trapped within the mould once it has filled, probably due to entrainment, or from gas pore growth as dissolved gas precipitates from solution during solidification [1].

Much work has taken place in the last 20 years to build solver technologies and host software to enable foundry engineers to design manufacturing solutions which eliminate such defects. Computational methods are typically based upon one of two families of techniques:

a) Finite volume methods using structured meshes, from which complex geometries are 'carved out' fairly straightforwardly – when meshes are fine enough then these methods resolve the geometric details well enough and the solvers work extremely well, and

b) Finite element methods, often embedding some form of local conservation - such methods obviously catch the geometric details well from the outset, but adequate mesh generation is non-trivial and runtimes tend to be somewhat larger.

Both methods use versions of the Volume-of-Fluid (VOF) technique to capture the emerging free surface. However, this is complicated within complex geometries and so numerical filters are frequently used to ensure the techniques are stable and robust under most conditions. This can have the effect of dampening out the free surface development; this may not be important for many applications where quiescent flow is targeted. However, there are situations where capturing the details of the free surface behaviour is vital. Moreover, the combination of a free surface solver with the moving liquid-solid boundary during solidification is also very difficult to handle and so most codes separate out these tasks, rationalising that the mould filling is a short time process whilst relatively speaking, solidification is a long time process. Hence, a simulation might initially involve free surface flow alone for the short filling stage, followed by residual flow, heat transfer and solidification for the remainder of the simulated time.

However, when working with some difficult to cast alloys for high specification applications solidification can occur during mould filling. Moreover, since some emerging processes are utilising rotating moulds then the circumferential forces are significant and have to be accounted for. In this context the capture of the free surface is a genuine challenge. Methods that work well for relatively quiescent mould filling, such as, van Leer [2] based surface capturing algorithms smear unacceptably. Methods which are better at surface capture, such as, donor-acceptor algorithms are much more sensitive to mesh quality and so make demands on the element quality throughout the whole mesh – one poor quality element can cause the whole procedure to fail [3].

This contribution will show some validation results in simulating the filling behaviour of a liquid in rotating moulds. The model is implemented within PHYSICA [4] where the numerical procedures are based upon finite volume methods on unstructured heterogeneous meshes for complex 3D geometries [5] and with scalable speed-up in parallel [6].

Governing Equations

In most cases the liquid metal (and possibly the air being expelled as the mould fills) is represented as a Newtonian fluid by the Navier-Stokes equations:
a) for fluid momentum

$$\frac{\partial(\rho \underline{u})}{\partial t} + \nabla.(\rho \underline{\underline{u}}\, \underline{u}) = \nabla.\left(\mu_{eff} \nabla \underline{u}\right) + \underline{S}_u - \nabla p \qquad (1)$$

b) for mass conservation

$$\frac{\partial \rho}{\partial t} + \nabla.\left(\rho \underline{u}\right) = S_m \qquad (2)$$

where $\underline{u}$ is the fluid mixture velocity, ρ is the fluid mixture density, p is pressure and μ_{eff} is the effective viscosity. These equations may well be augmented by turbulence models to calculate

the effective viscosity – although, there is much debate about their efficacy in the context of many mould filling scenarios where the opportunity to develop turbulence structures within the physical timeframe is very limited.

The governing equations are solved in a non-inertial reference frame, where the co-ordinate system moves with the rotating equipment. To account for the acceleration of the fluid the centrifugal and coriolis forces enter the momentum equations as fictitious forces. The velocity of the fluid relative to the co-ordinate system can be expressed as;

$$\underline{u}_r = \underline{u} - (\underline{\Omega} x \underline{r}) \tag{3}$$

Substituting (3) into (1) and re-arranging the left hand side of (1) can be written as;

$$\frac{\partial}{\partial t}\left(\rho \underline{u}_r\right) + \nabla.\left(\rho \underline{u}_r \underline{u}_r\right) + \rho\left(2\underline{\Omega} x \underline{u}_r + \underline{\Omega} x (\underline{\Omega} x \underline{r})\right) \tag{4}$$

and equation (2) as;

$$\frac{\partial \rho}{\partial t} + \nabla.\left(\rho \underline{u}_r\right) = S_m \tag{5}$$

When the fluid is rotating at the same velocity as the rotating frame the forces should balance and the relative velocity is equal to zero. The differencing scheme employed in the numerical discretisation of the governing equations is crucial to ensuring the balance of forces and hence the correct time period for a stationary fluid to achieve its rotational velocity. A first order scheme is not sufficient and a higher order scheme such as, SMART [7] is required.

Almost all viable simulation tools for the simulation of free surface flows in shape casting use a fixed grid approach as defined by the mould geometry. They either employ the concept of volume of fluid (VOF), originally proposed by Hirt and Nichols [8], to track the interface and to reconstruct geometrically its location, or the equation for the advection of the scalar,

$$\frac{\partial \phi}{\partial t} + \nabla \cdot (\phi \underline{u}_r) = S_\phi \tag{6}$$

is solved numerically and then the interface is captured as a discontinuity in the solution field via an appropriate non-diffusive scheme (e.g. van Leer [2]. in the SEA algorithm). The VOF tracking method leads to a sharp interface, but it is not guaranteed to conserve mass. In contrast, the surface capturing approach, although conservative, is computationally more demanding and it suffers from numerical diffusion.

There are a host of workers who have essentially employed the VOF concept within algorithms using all kinds of combinations of finite element and finite volume methods. Since both methods require an explicit time stepping for accuracy, a stable solution is ensured only by using a small enough time step to satisfy the smallest CFL number in the mesh. There are now many useful tricks for ensuring this can be done efficiently. The method employed in this paper is essentially the FV-UM scheme of Pericleous [9], which uses as part of the SEA TVD capturing scheme, the GALA scheme developed by Spalding [10] combined with a Donor Acceptor [11] to ensure the interface remains sharp as it convects through a fixed mesh.

Model Results vs. Experimental Measurements

A series of water model experiments have been performed and recorded using high-speed video image capture. The objective was to validate and refine the computational model predictions using repeatable high quality experimental data.

Experimental equipment

A transparent cylinder was used to represent a casting mould, whilst allowing clear video footage of the movement of the liquid inside to be acquired. The bottom of the cylinder was sealed with a metal stop, which also acted as an attachment to allow the cylinder to be rotated. The cylinder was filled by use of a funnel, the size of which had been determined to replicate the pouring time of a centrifugal casting process. Water at room temperature was used to fill the cylinder, which was dyed red to aid visualization when required. An adjustable speed motor was used to spin the cylinder, in conjunction with a digital tachometer to measure of rotational velocity. A high speed camera was used to view the experiment at 500 frames per second, at 498×332 resolution. In addition, further experiments were undertaken with a round conduit containing a radiused bend attached to the bottom of the funnel to allow the profile of the liquid to be studied.

Characterising the fluid flow

Initial experiments to characterise the flow of the liquid from a funnel were undertaken so that it could be compared to the pouring profile of metal from a crucible, such that later analysis of the filling could be completed accurately. The flow was set against a gridded background and recorded with the camera set back as far as possible from the flow so that errors of parallax could be minimised. At frequent intervals in the pour, discrete fluctuations of the flow were tracked in a viewing program. These were scaled to SI units then converted to Cartesian coordinates by trilateration, shown in Figure 1. The coordinates were plotted to obtain parabolic lines of best fit,

$$y = ax^2 + bx + c \tag{7}$$

By substituting values of the equation and its derivatives into itself, the form was translated to give simple uniform acceleration equations of motion.

$$s = vt - \frac{1}{2}gt \tag{8}$$

These equations were resolved so that the velocity of flow at the outlet was found for the inclination angle, θ, given by the parabolic equation, Figure 2. While the inclination angle remained constant for an individual experiment, the outlet velocity of the funnel changed with its hydraulic head of water. By plotting the measured outlet velocities against time, t, a full profile of the pour was achieved, described by (9), shown in Figure 3.

$$0.3 + 1.1255\cos\left(\frac{243\pi t^5}{16}\right) - \frac{t}{5} \tag{9}$$

This pour profile was completed by adding an expression for fluctuation of the outlet diameter, by tracking the amplitude of the pour close to the outlet.

$$\phi = 7 + (\pi + 1.5\theta)\sin(300t) \tag{10}$$

With a set of equations fully characterising the pour profile of the funnel, an experiment was run to measure the volume of liquid having been poured into the test cylinder against the volume predicted by the model. Figure 4 shows the percentage difference between the volumes measured in the experiment, against the volumes predicted by the mass flow rate. The two lines show how, by using the variable mass flow rate of equation (9), a much reduced error in describing the mass flux of the pour was obtained, compared to a fixed mass flow rate. The residual difference can be accounted for by the inclusion of bubbles within the pour, and error in measurement of the height of the volume within the cylinder.

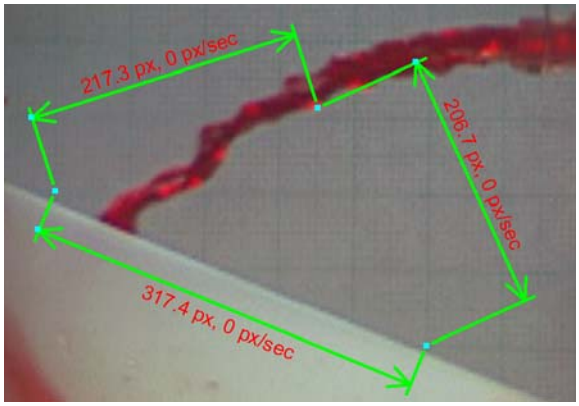

Figure 1 : Trilateration of liquid flow at 1 second

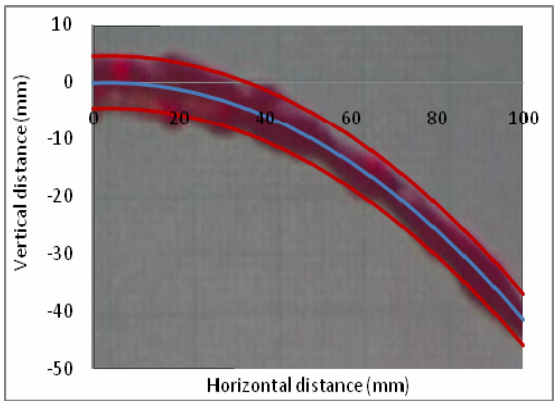

Figure 3: Pour velocity against time

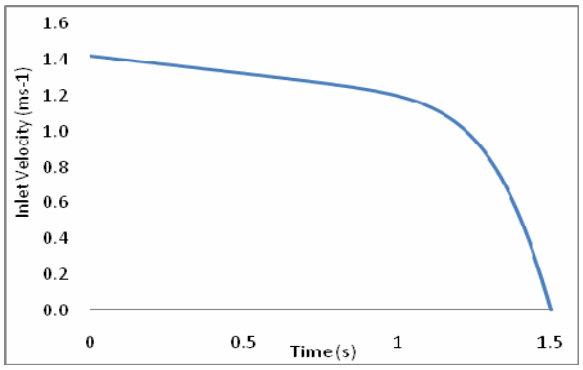

Figure 2: Parabolic line of best fit at 1 second

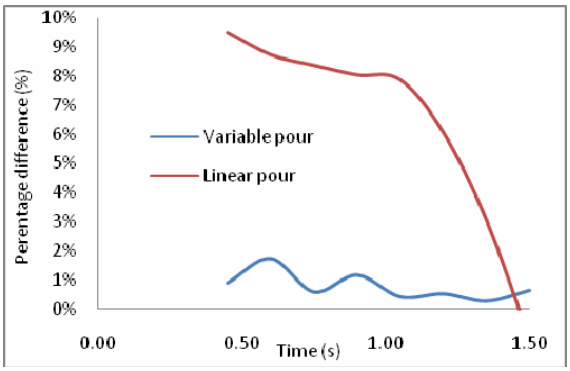

Figure 4: Percent difference between predicted and measured mass flux as a function of time

Vortex formation

With the centrifugal effect of the rotation being critical to the filling of the cast part, it is essential that the model is carefully calibrated, so that the rotational velocity, ω, at the mould wall is correctly radiated through the fluid to the centre of rotation. Experiments were filmed in which the cylinder, filled with 67ml of still water, was instantly accelerated to 400rpm by use of the motor. At time intervals of 5 seconds, the profile of the free surface was plotted, so that the height, h, of the free surface could be determined along the radius, r, of the cylinder. The height was compared to the theoretical height of the steady state vortex, given by

$$h(r)=r^2\frac{\omega^2}{2g}+h(0) \qquad (11)$$

It was shown that the theoretical height of the steady state vortex, given by equation (11), at $r=0$ mm would be 22.4 mm, with the height at r=22 mm being 65.7 mm. In comparison to Figure 5, it can be seen that the transient state at 30s is some way below the theoretical ideal, and would appear to reach a steady state some way below the theoretical maximum. By taking the derivative of the parabolic form in Equation (11), it is possible to estimate the rotational velocity of the fluid at a given radius.

$$\frac{\delta h}{\delta r} = 2r\frac{\omega^2}{2g}, \qquad \omega = \sqrt{\frac{hg}{r}} \tag{12}$$

The change in the velocity profile of the free surface against time can be seen in Figure 6. It shows that while the fluid close to the boundary wall quickly accelerates towards 400rpm as predicted by a no slip condition, the velocity is not passed fully to the centre of rotation. Both Figure 5 and Figure 6 suggest the water is coming towards a steady state at a rotational velocity below the expected value.

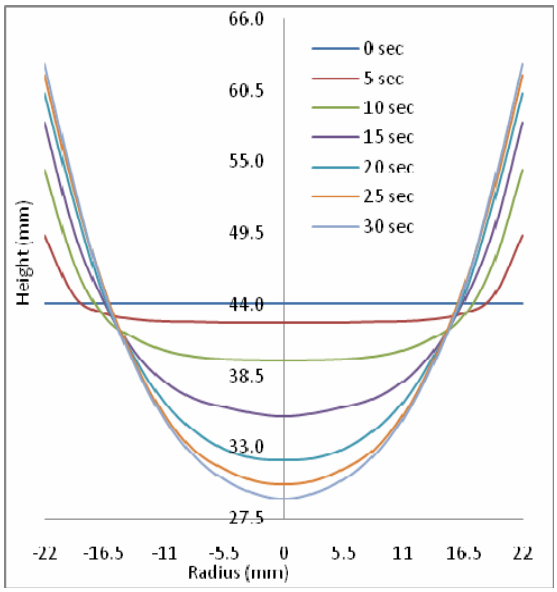

Figure 5: Height of forced vortex free surface against time

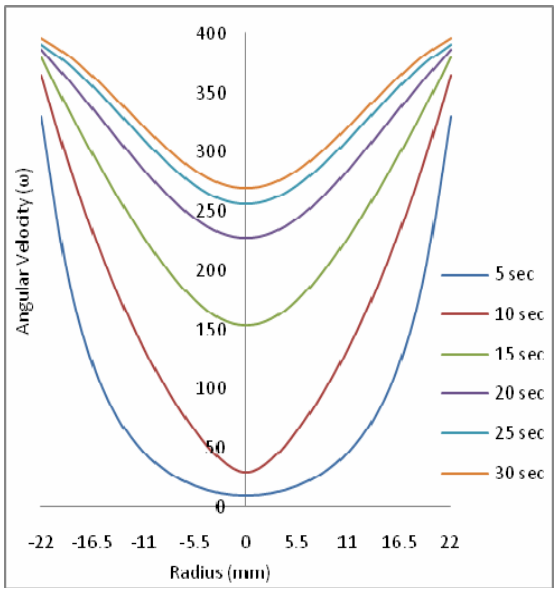

Figure 6: Inferred rotational velocity at the free surface

For valid model predictions, it is important that the centrifugal forces balance with convective forces. If a first order differencing scheme is employed the model achieves rotational velocity within seconds. Employing a higher order differencing scheme, SMART, gave simulated development of rotational fluid velocity in good agreement with experimental observed values. Figure 7 shows how the model simulates the height of the vortex between 0 and 64 seconds, in comparison to the height measured in the experiment. It can be seen that the profiles of the two are extremely similar.

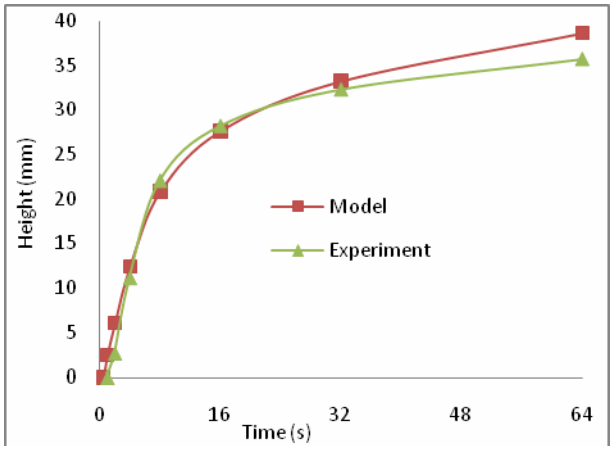

Figure 7: Extension of the height of the forced vortex

Fluid Film

In the simulation, an important factor in the behaviour of the fluid within the model is the interaction at the boundary between the mould and the liquid. To test the validity of the model, the cylinder was filled by use of the funnel, with the conduit attached to the end, so that the liquid was directed at the wall. Video footage was viewed at $\frac{1}{100}$second intervals to show the relative spread of the fluid film at these times, Figure 8, Figure 9 and Figure 10. By tracing the boundary of the fluid and transposing the outline Cartesian coordinates defining the film boundary were obtained. These coordinates were converted to curvilinear coordinates and plotted to correspond to the fluid travelling around the curved surface of the cylinder.

Figure 8: 0.02seconds

Figure 9: 0.03 seconds

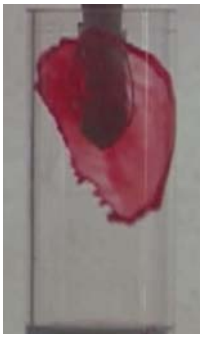

Figure 10: 0.04seconds

Initial results were analysed to find the attachment to the wall. It was noted that the trailing edge of the film boundary formed something of a characteristic angle until disturbed by the leading edge of the film on completion of a full rotation, Figure 11. The angle was found to be related to the rotational velocity and the attachment of the fluid to the wall. A fluid showing strong attachment to the wall would hold its height and offer a small angle, while fluid showing little attachment would tend to fall to the bottom of the cylinder before completing a full rotation, giving a large angle. The angle of the fluid hitting the wall of the cylinder at 400rpm was measured at 51.6°; this was compared to the model to allow the fluid coupling and attachment to the wall to be validated.

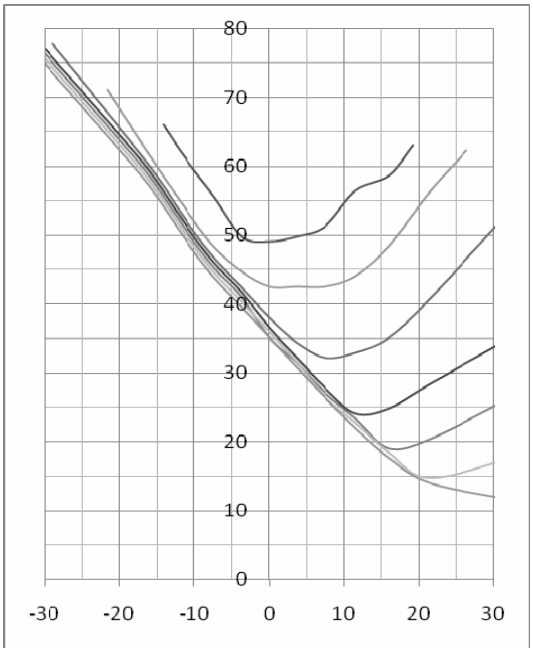

Figure 11: Lower boundary of fluid film at one hundredth of a second interval

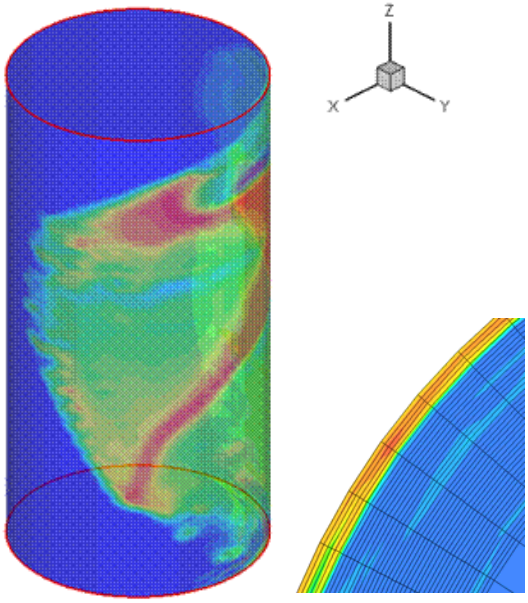

Figure 12: Simulated fluid attachment, showing characteristic angle and film thickness

By plotting the upper and lower boundaries of the fluid film at frequent time intervals in the experiment, it was possible to perform a double integration of the film boundaries, to define an accurate value for the film area. The previously established mass flow rate was used to determine an average thickness for the given film area, by plotting the change in film area with the mass flux. The water model calculated the average film thickness as 0.54mm. This was compared to simulation, Figure 12, which gave the thickness as between 0.25mm and 0.5mm, but showing areas along the leading edge of the film to be thicker than this. Given the thicker areas of the fluid front, the average thickness of the water was likely to be lower, in keeping with the simulated values.

Conclusions

This contribution has described a number of the enhancements required to enable conventional free surface algorithms to capture the details of the flow during the filling stage of centrifugal casting. Validation of these enhancements has been performed against a series of water model experiments. The enhancements have allowed the accurate prediction of the initial fluid film and the vortex formation. The aim is to use the model to correctly resolve the entrapment, coalescence, fragmentation and transport of air bubbles during centrifugal casting.

References

[1] J Campbell, Castings, 2nd Edition, Butterworth-Heinemann, 2003

[2] B van Leer, Towards the ultimate conservation difference scheme. IV a new approach to numerical convection, *J Comp Phys*, Vol. **23**, pp. 276-299 (1979)

[3] S M Bounds, A Computational Model for Defect Prediction in Shape Castings Based on the Interaction of Free Surface Flow, Heat Transfer, and Solidification Phenomena, *Metallurgical and Materials Transactions B*, Vol. **31B,** pp.515-527 (2000)

[4] PHYSICA, see http://physica.co.uk

[5] K Pericleous, G L Moran, S M, Bounds, P, Chow, and M Cross, Three Dimensional Free Surface Modelling in an Unstructured Mesh Environment for Metal Processing Applications. *Applied Math Modelling*, Vol. **22**, pp.895-906, (1998)

[6] K McManus, A J Williams, M Cross, T N Croft, and C Walshaw, Assessing the parallel performance of multi-physics tools for modelling of solidification and melting processes, *Intl Jnl High Perf Comp Applns*, **19**, 1-27 (2005)

[7] P H Gaskell and A K C Lau, Curvature-compensated convective transport: SMART, A new boundedness-preserving transport algorithm, *IJNME*, **8**, pp. 617-641 (1988)

[8] C W Hirt and B D Nichols, Volume of fluid (VOF) method for the dynamics of free boundaries, *J. Comp. Phys*. **39**, pp 201-225 (1981).

[9] K Pericleous, Three-dimensional free surface modelling in an unstructured mesh environment for metal processing applications, *Appl Math Modelling*, **22**, pp 895-906 (1998)

[10] D B Spalding, Mathematical modelling of fluid mechanics, heat transfer and chemical reaction processes, *Report HTS – 80-1*, Mech Engg Dept, Imperial College London (1980)

[11] J B Ramshaw and J A Trapp, A numerical technique for low speed homogeneous two phase flow with a sharp interface*, Journal of Computational Physics*, **21,** pp 438-453 (1976)